

ChemComm

Directed selective self-assembly of a ring-in-ring complex

Ross S. Forgan,^a Douglas C. Friedman,^a Charlotte L. Stern,^a Carson J. Bruns^a and J. Fraser Stoddart^a

Supplementary Information

^aCenter for the Chemistry of Integrated Systems
Department of Chemistry
Northwestern University
Evanston, IL 60208
USA

E-mail: stoddart@northwestern.edu

S1. Compounds used in this Study

The compounds displayed in Figure S1 were prepared or discussed in this study.

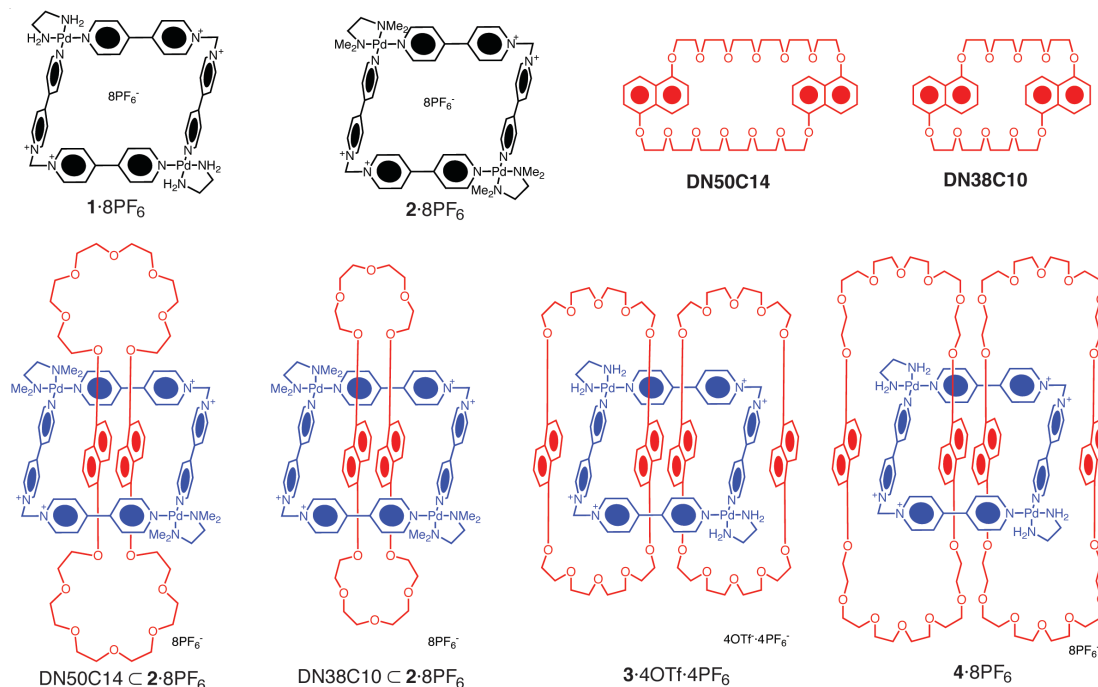


Fig S1. Structural formulae of compounds prepared or described in this investigation.

Throughout the document, ethylenediamine is abbreviated to “en” and tetramethylethylenediamine to “tmeda”.

S2. Synthesis

All reagents were purchased from commercial suppliers (Aldrich or Fisher) and used without further purification. 1,1'-Methylenebis-4,4'-bipyridinium bis(hexafluorophosphate),^{S1} bis-1,5-dioxynaphtho[50]crown-14 (DN50C14)^{S2} and bis-1,5-dioxynaphtho[38]crown-10 (DN38C10)^{S3} were prepared according to literature procedures. Nuclear magnetic resonance (NMR) spectra were recorded at 298 K unless stated otherwise on Bruker Avance III 500 and 600 MHz spectrometers, with working frequencies of 499.373 and 600.168 MHz for ¹H, and 125.579 and 150.928 MHz for ¹³C nuclei, respectively. Diffusion Ordered Spectroscopy (DOSY) was

performed on a Bruker Avance 800 MHz spectrometer using a triple-axis gradient TCI probe. All ^{13}C spectra were recorded with the simultaneous decoupling of proton nuclei. Chemical shifts are reported in ppm relative to the signals corresponding to the residual non-deuterated solvents (1.94 ppm for MeCN). Electrospray Ionisation (ESI) mass spectra were obtained on a Agilent 6210 LC-TOF high resolution mass spectrometer. X-Ray diffraction data for $2\cdot 8\text{PF}_6$ and $4\cdot 8\text{PF}_6$ were collected on a Bruker Kappa diffractometer, equipped with a Cu $K\alpha$ sealed-tube source and an APEX II CCD detector. X-Ray diffraction data for $\text{DN50C14} \subset 2\cdot 8\text{PF}_6$ were collected on a Bruker Kappa diffractometer, equipped with a Mo $K\alpha$ sealed-tube source and an APEX II CCD detector. UV/Vis spectra were collected on a Shimadzu UV-3600 UV-Vis-NIR spectrophotometer.


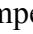
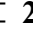
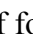
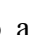
Metallocycle $2\cdot 8\text{PF}_6$. 1,1'-Methylenebis-4,4'-bipyridinium bis(hexafluorophosphate) (12.3 mg, 20 μmol), $[\text{Pd}(\text{tmeda})\text{Cl}_2]$ (5.9 mg, 20 μmol) and AgPF_6 (10.2 mg, 40 μmol) were combined in CD_3CN (1 ml) and stirred thoroughly for 15 mins. The white precipitate (AgCl) was removed by filtration and the pale yellow solution was analysed by ^1H NMR spectroscopy. ^1H NMR (CD_3CN , 293 K, 500 MHz) δ 9.10 (d, $J = 6.7$ Hz, 4H), 9.05 (d, $J = 7.0$ Hz, 4H), 8.36 (d, $J = 7.0$ Hz, 4H), 7.98 (d, $J = 6.7$ Hz, 4H), 7.07 (s, 2H), 3.03 (s, 4H), 2.66 (s, 12H). ^{13}C NMR (CD_3CN , 293 K, 125 MHz) δ 154.1, 151.8, 145.9, 143.7, 127.0, 125.9, 76.8, 62.4, 50.2. Single crystals, suitable for X-ray analysis, were grown by vapour diffusion of Et_2O into the CD_3CN solution over 3 days. Crystal data: $\text{C}_{66}\text{H}_{90}\text{F}_{48}\text{N}_{16}\text{O}_8\text{P}_8\text{Pd}_2$, $M_r = 2496.10$, triclinic, space group = $P-1$, $a = 8.719(2)$, $b = 13.919(3)$, $c = 22.991(6)$ Å, $\alpha = 67.791(20)$, $\beta = 79.998(19)$, $\gamma = 76.088(19)^\circ$, $V = 2496.7(10)$ Å³, $T = 100(2)$ K, $Z = 1$, 6170 reflections measured, 3582 unique ($R_{\text{int}} = 0.1956$), $R_1 (F^2 > 2\sigma F^2) = 0.0766$.

Ring-in-ring complex $\text{DN50C14} \subset 2\cdot 8\text{PF}_6$. 1,1'-Methylenebis-4,4'-bipyridinium bis(hexafluorophosphate) (6.1 mg, 10 μmol), $[\text{Pd}(\text{tmeda})\text{Cl}_2]$ (2.9 mg, 10 μmol), DN50C14 (4.1 mg, 5 μmol), and AgPF_6 (5.1 mg, 20 μmol) were combined in CD_3CN (1 ml) and stirred thoroughly for 15 mins. The white precipitate (AgCl) was removed by filtration and the purple solution analysed by ^1H NMR spectroscopy. ^1H NMR (CD_3CN , 233 K, 600 MHz) δ 9.91 (d, $J = 6.1$ Hz, 2H), 9.52 (d, $J = 6.4$ Hz, 2H), 9.32 (d, $J = 6.4$ Hz, 2H), 9.22 (d, $J = 5.7$ Hz, 2H), 9.18 (d, $J = 6.4$ Hz, 2H), 9.05 (d, $J = 6.4$

Hz, 2H), 8.88 (d, $J = 6.2$ Hz, 2H), 8.85 (d, $J = 6.2$ Hz, 2H), 8.78 (d, $J = 6.4$ Hz, 2H), 8.75 (d, $J = 6.4$ Hz, 2H), 8.56 (d, $J = 6.4$ Hz, 2H), 8.40 (d, $J = 6.4$ Hz, 2H), 7.30 (d, $J = 5.8$ Hz, 2H), 7.26 (d, $J = 6.4$ Hz, 2H), 7.08 (d, $J = 6.4$ Hz, 2H), 6.98 (d, $J = 6.4$ Hz, 2H), 6.83 (d, $J = 14.2$ Hz, 2H), 6.75 (d, $J = 14.2$ Hz, 2H), 5.91 (d, $J = 7.7$ Hz, 2H), 5.76 (d, $J = 7.7$ Hz, 2H), 5.71 (t, $J = 7.7$ Hz, 2H), 5.24 (t, $J = 7.7$ Hz, 2H), 4.50–2.50 (m, 84H), 3.78 (d, $J = 8.2$ Hz, 2H), 3.03 (d, $J = 8.2$ Hz, 2H). ^{13}C NMR (CD_3CN , 233 K, 150 MHz) δ 152.9, 152.8, 152.7, 152.6, 152.4, 152.0, 151.0, 150.1, 149.1, 146.5, 145.7, 144.9, 144.5, 143.9, 140.4, 128.4, 127.6, 127.1, 126.4, 126.1, 125.5, 125.2, 125.1, 124.9, 124.7, 124.0, 123.5, 110.0, 108.7, 104.2, 103.6, 77.1, 72.4, 72.2, 71.5, 70.8, 69.6, 69.5, 69.2, 68.4, 68.0, 68.0, 65.8, 62.8, 62.7. UV/Vis (CD_3CN , 12.5 mM) $\lambda_{\text{max}} = 510$ nm. Single crystals, suitable for X-ray analysis, were grown by vapour diffusion of Et_2O into the CD_3CN solution over 3 days. Crystal data: $\text{C}_{117}\text{H}_{162.5}\text{F}_{48}\text{N}_{18.5}\text{O}_{15.5}\text{P}_8\text{Pd}_2$, $M_r = 3448.72$, monoclinic, space group = $P2_1/n$, $a = 18.2943(3)$, $b = 17.8612(3)$, $c = 23.4887(3)$ Å, $\beta = 92.936(1)^\circ$, $V = 7646.2(2)$ Å³, $T = 100(2)$ K, $Z = 2$, 23118 reflections measured, 13668 unique ($R_{\text{int}} = 0.0630$), $R_1 (F^2 > 2\sigma F^2) = 0.0781$. Group anisotropic displacement parameters were refined for disordered fluorines. Bond restraints were imposed on the disordered C48b.

[3]Catenane 4·8PF₆. 1,1'-Methylenebis-4,4'-bipyridinium bis(hexafluorophosphate) (6.1 mg, 10 μmol), $[\text{Pd}(\text{en})\text{Cl}_2]$ (2.4 mg, 10 μmol), DN50C14 (8.2 mg, 10 μmol) and AgPF_6 (5.1 mg, 20 μmol) were combined in CD_3CN (1 ml) and stirred thoroughly for 15 mins. The white precipitate (AgCl) was removed by filtration and the purple solution analysed by ^1H NMR spectroscopy. ^1H NMR (CD_3CN , 233 K, 600 MHz) δ 9.65 (br s, 2H), 9.47 (br s, 2H), 9.23 (br s, 3H), 9.11 (br d, $J = 5.6$ Hz, 2H), 8.79 (m, 4H), 8.30–8.60 (m, 7H), 8.27 (br s, 1H), 8.12 (br d, $J = 6.1$ Hz, 1H), 8.07 (br s, 1H), 7.83 (br s, 1H), 7.76 (br s, 2H), 7.61 (br d, $J = 6.1$ Hz, 1H), 7.38 (d, $J = 14.7$ Hz, 1H), 7.05–7.30 (m, 9H), 6.50–6.80 (m, 12H), 6.37 (br d, $J = 8.0$ Hz, 1H), 6.30 (br d, $J = 5.7$ Hz, 1H), 6.24 (br t, $J = 8.0$ Hz, 1H), 6.17 (br m, 3H), 6.05 (br d, $J = 6.0$ Hz, 1H), 5.65 (br d, $J = 7.6$ Hz, 1H), 5.60 (br t, $J = 7.6$ Hz, 1H), 5.48 (br d, $J = 7.6$ Hz, 1H), 5.24 (br m, 2H), 5.11 (br m, 3H), 4.97 (br m, 1H), 4.74 (br s, 2H), 3.20–4.60 (br m, 125H), 2.98 (br m, 4H), 2.85 (br s, 6H), 2.75 (br s, 8H). UV/Vis (CD_3CN , 6.25 mM) $\lambda_{\text{max}} = 510$ nm. Single crystals, suitable for X-ray diffraction, were grown by vapour diffusion of Et_2O into the CD_3CN solution over 3 days. Crystal data: $\text{C}_{297}\text{H}_{380}\text{F}_{96}\text{N}_{38}\text{O}_{64}\text{P}_{16}\text{Pd}_4$, $M_r = 8251.51$, triclinic, space group = $P-1$, $a = 19.0335(6)$,

$b = 21.1652(7)$, $c = 26.7873(8)$ Å, $\alpha = 72.664(2)$, $\beta = 79.146(2)$, $\gamma = 71.025(2)$ °, $V = 9691.2(5)$ Å³, $T = 293(2)$ K, $Z = 1$, 27227 reflections measured, 17398 unique ($R_{\text{int}} = 0.0787$), $R_1 (F^2 > 2\sigma F^2) = 0.1125$. Chemically equivalent, but not symmetry equivalent O15–C135 atoms were restrained so that bond distances and angles were similar to O1–C91. Rigid bond restraints (esd 0.01) were imposed on the displacement parameters as well as restraints on similar amplitudes (esd 0.05) separated by less than 1.7 Å on O15–C1935. The hydrogen atoms on the water molecules were not located.

Ring-in-ring complex DN38C10  2·8PF₆. 1,1'-Methylenebis-4,4'-bipyridinium bis(hexafluorophosphate) (6.1 mg, 10 μmol), [Pd(tmeda)Cl₂] (2.9 mg, 10 μmol), DN38C10 (3.2 mg, 5 μmol), and AgPF₆ (5.1 mg, 20 μmol) were combined in CD₃CN (1 ml) and stirred thoroughly for 15 mins. The white precipitate (AgCl) was removed by filtration and the purple solution analysed by ¹H NMR spectroscopy. ¹H NMR (CD₃CN, 233 K, 600 MHz) δ 9.55 (d, $J = 6.4$ Hz, 2H), 9.46 (br s, 4H), 9.35 (d, $J = 6.4$ Hz, 2H), 8.94 (br s, 4H), 8.93 (d, $J = 6.4$ Hz, 2H), 8.89 (d, $J = 6.4$ Hz, 2H), 8.80 (br d, $J = 6.4$ Hz, 2H), 8.70 (br d, $J = 6.4$ Hz, 2H), 8.54 (br d, $J = 6.4$ Hz, 2H), 8.20 (br d, $J = 6.4$ Hz, 2H), 7.42 (br d, $J = 6.4$ Hz, 2H), 7.34 (br d, $J = 6.4$ Hz, 2H), 7.15 (br d, $J = 6.4$ Hz, 2H), 6.87 (d, $J = 14.8$ Hz, 2H), 6.77 (br d, $J = 6.4$ Hz, 2H), 6.74 (d, $J = 14.8$ Hz, 2H), 5.95 (d, $J = 7.8$ Hz, 2H), 5.67 (d, $J = 7.8$ Hz, 2H), 5.61 (t, $J = 7.8$ Hz, 2H), 5.22 (t, $J = 7.8$ Hz, 2H), 4.52 (t, $J = 11.2$ Hz, 2H), 4.36 (m, 2H), 3.50–4.25 (m, 64H), 3.77 (d, $J = 7.8$ Hz, 2H), 3.12 (d, $J = 7.8$ Hz, 2H), 3.00 (br s, 12 H), 2.74 (br s, 16H). UV/Vis (CD₃CN, 25 mM) $\lambda_{\text{max}} = 510$ nm. In repeated experiments, the ¹H NMR spectrum showed significant signals corresponding to the free metallocyclophane 2·8PF₆, but no excess of DN38C10. The very low solubility of DN38C10 in CD₃CN, combined with fact that, at room temperature, the formation of DN38C10  2·8PF₆ is not favoured, result in the loss of large amounts of DN38C10 in the filtration step. At 233 K, formation of DN38C10  2·8PF₆ is favoured (see Section S4) and the remaining DN38C10 in solution forms the ring-in-ring complex. Dilution of the mixture to a concentration where all starting materials are soluble in CD₃CN, however, perturbs the equilibrium of formation of DN38C10  2·8PF₆, resulting in an ¹H NMR spectrum consisting of 2·8PF₆ and DN38C10, but no DN38C10  2·8PF₆. Signals which could correspond to a [3]catenane were not detected in any of the

spectra. These observations demonstrate that, despite the fact that assembly of the ring-in-ring complex $\text{DN38C10} \subset 2 \cdot 8\text{PF}_6$ is not as favourable as $\text{DN50C14} \subset 2 \cdot 8\text{PF}_6$, the use of the Pd(tmeda) complex again precludes any formation of a [3]catenane. The problems encountered with the low solubility of DN38C10 in CD_3CN , coupled with the disfavouring of assembly of $\text{DN38C10} \subset 2 \cdot 8\text{PF}_6$ at room temperature, meant that it was not possible to isolate any pure $\text{DN38C10} \subset 2 \cdot 8\text{PF}_6$ for further analysis.

S2. NMR Characterisation of $\text{DN50C14} \subset 2 \cdot 8\text{PF}_6$

The dynamic nature of both the Pd-N bond and the complex formed between DN50C14 and $2 \cdot 8\text{PF}_6$ was evident in the variable temperature ^1H NMR spectra (Figure S2) recorded on a mixture of the two. While significant line broadening was apparent at room temperature, the resonances become well resolved as soon as the temperature is lowered to 233 K.

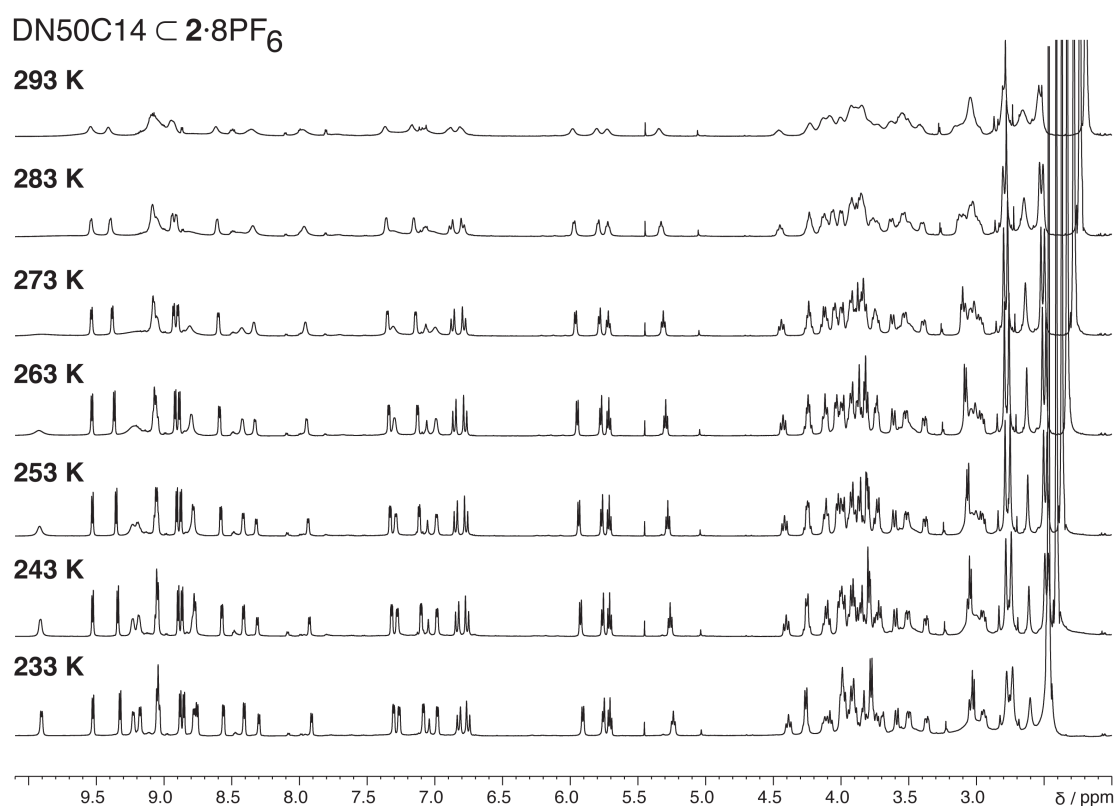


Fig S2. Stacked plot of variable temperature 600 MHz ^1H NMR spectra of an equimolar mixture of DN50C14 and $2 \cdot 8\text{PF}_6$ recorded in CD_3CN at 10 K intervals from 233 K to 293 K.

It was possible to assign (Figure S3) fully the ^1H NMR spectrum of $\text{DN50C14} \cdot 2\cdot 8\text{PF}_6$ recorded in CD_3CN at 233 K by employing the range of 2D techniques described below.

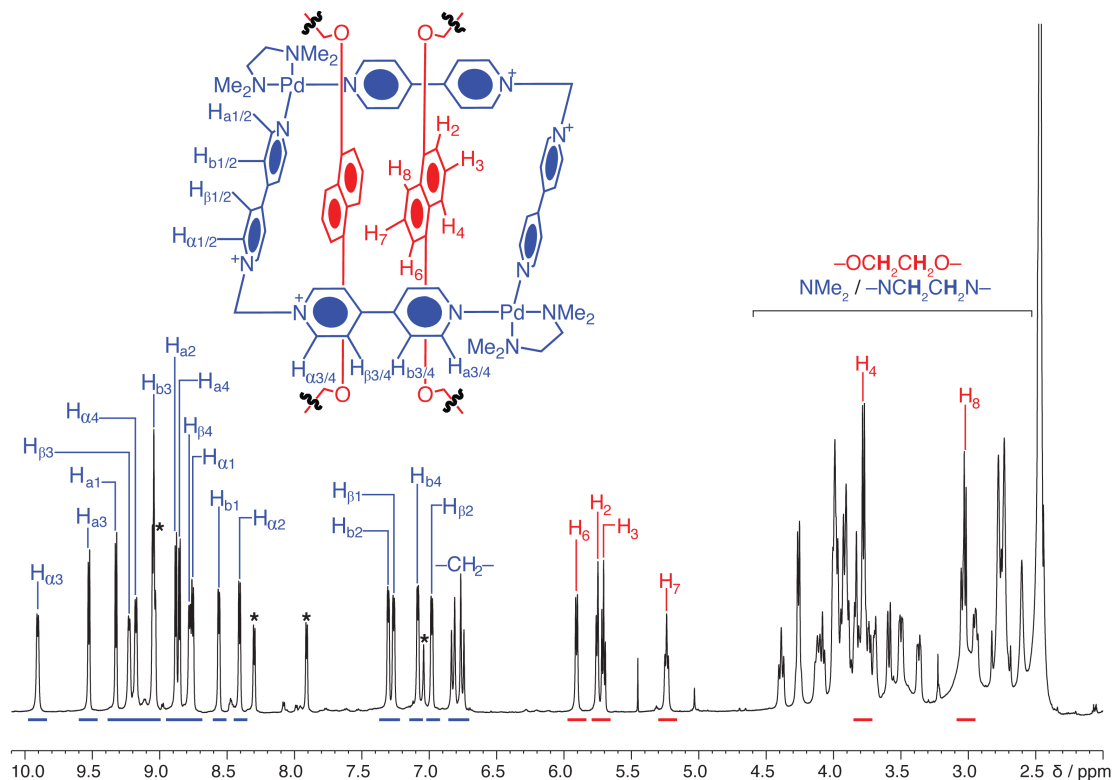


Fig S3. ^1H NMR spectrum (600 MHz, 233 K, CD_3CN) of $\text{DN50C14} \cdot 2\cdot 8\text{PF}_6$. Resonances marked with an asterisk (*) correspond to signals for the free square $2\cdot 8\text{PF}_6$. To assist with characterisation, the protons (blue) of the pyridinium units of the 1,1'-methylenebis-4,4'-bipyridinium ligand are labelled as H_α and H_β , respectively, while the protons of the pyridine units coordinated to the Pd^{II} cations are labelled as H_a and H_b . The diastereotopic protons of the methylene unit are labelled as $-\text{CH}_2-$. The six aromatic protons of the dioxynaphthalene (DNP) units (red) are labelled H_2 , H_3 , H_4 , H_6 , H_7 and H_8 , according to their position on the aromatic ring system.

The low overall C_i symmetry of $\text{DN50C14} \cdot 2\cdot 8\text{PF}_6$ leads to a large number of resonances being associated with this ring-in-ring complex. This level of complexity, with 16 downfield resonances for the bipyridinium protons, represents a significant reduction in symmetry when compared to components alone in solution. Careful analysis of the 1D ^1H NMR spectrum, in conjunction with the multidimensional techniques below, allowed us to have a great deal of confidence in the assignments recorded in Figure S3.

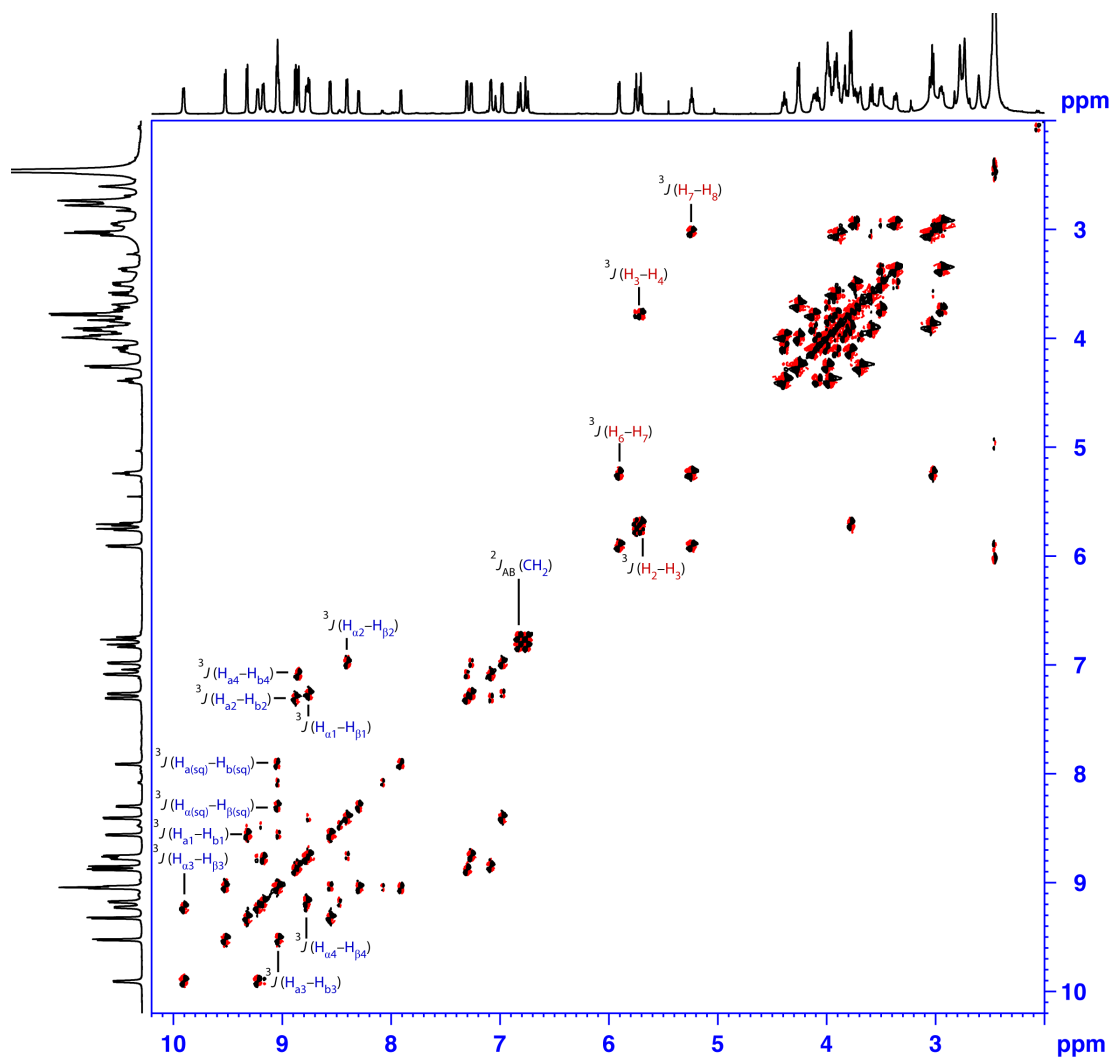


Fig S4. ^1H - ^1H gDQF-COSY NMR spectrum (600 MHz, 233 K, CD_3CN) of $\text{DN50C14} \cdot 2 \cdot 8\text{PF}_6$, with selected correlations labeled.

From the ^1H - ^1H gDQF-COSY NMR spectrum recorded in CD_3CN at 233 K (Figure S4), it was possible to identify 3J correlations between the eight pairs of H_α and H_β protons and H_a and H_b protons of the 1,1'-methylenebis-4,4'-bipyridinium ligand. Further assignment of these protons was carried out by examining the ^1H - ^1H NOESY NMR spectrum (Figure S5) recorded at 233 K. It showed through-space correlations between the methylene protons of 1,1'-methylenebis-4,4'-bipyridinium and the four adjacent H_α protons.

The COSY spectrum also allowed an unambiguous assignment to be made to the aromatic protons of the dioxynaphthalene units. Each of the six protons is symmetrically inequivalent, and as such two sets of correlated signals are observed,

corresponding to the H₂, H₃, H₄ grouping and the H₆, H₇, H₈ grouping on each side of the DNP unit. It was also possible to assign the H₄ and H₈ protons, which experience significant upfield shifts into the region dominated by –OCH₂CH₂O– resonances from the polyether chains of DN50C14. This shift is as a result of the shielding experienced by the protons, which point directly into the aromatic π-cloud of the 1,1'-methylenebis-4,4'-bipyridinium ligand. This hypothesis is further supported by the NOESY experiment, which shows through-space correlations between the pyridinium protons (H_α and H_β) and the H₆ and H₇ protons on the DNP ring system. Further confirmation of the H_α assignments were provided by the nOe correlations between the –CH₂– protons and each of the four H_α protons of the 1,1'-methylenebis-4,4'-bipyridinium ligand.

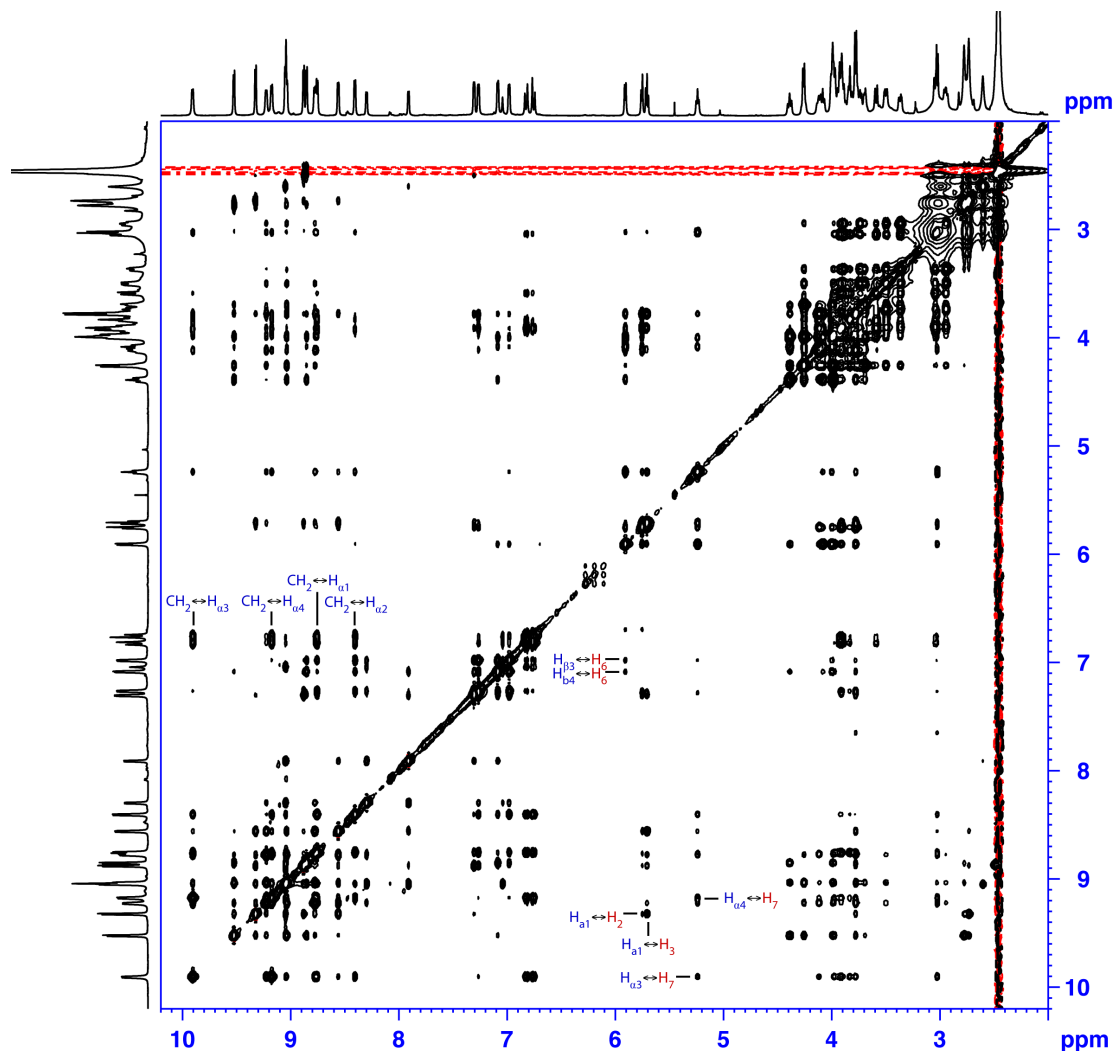


Fig S5. ¹H-¹H gNOESY NMR spectrum (600 MHz, 233 K, CD₃CN) of DN50C14 C 2·8PF₆, with selected correlations shown.

When examining the ^{13}C NMR spectrum (Figure S6) of $\text{DN50C14} \subset 2 \cdot 8\text{PF}_6$ it is noteworthy that the 1D ^{13}C spectrum contains 45 signals, i.e., exactly the number expected for the ring-in-ring complex: 10 for the aromatic carbon atoms of DN50C14, 12 for the polyether carbons of DN50C14, 21 for the 1,1'-methylenebis-4,4'-bipyridinium ligand and two for the carbon atoms of the tmeda ligand which constitute $2 \cdot 8\text{PF}_6$. Fourteen signals, assumed to be the aliphatic carbons of the polyether loops of DN50C14 and the tmeda ligand, are grouped ($\delta = 60\text{--}80$ ppm), while the remainder resonate further downfield. The 1D ^{13}C spectrum alone provides strong evidence for the formation of the ring-in-ring complex $\text{DN50C14} \subset 2 \cdot 8\text{PF}_6$ instead of the [3]catenane $4 \cdot 8\text{PF}_6$, which would be expected to have more peaks because of the inequivalence of the DNP units of each DN50C14 in the assembly.

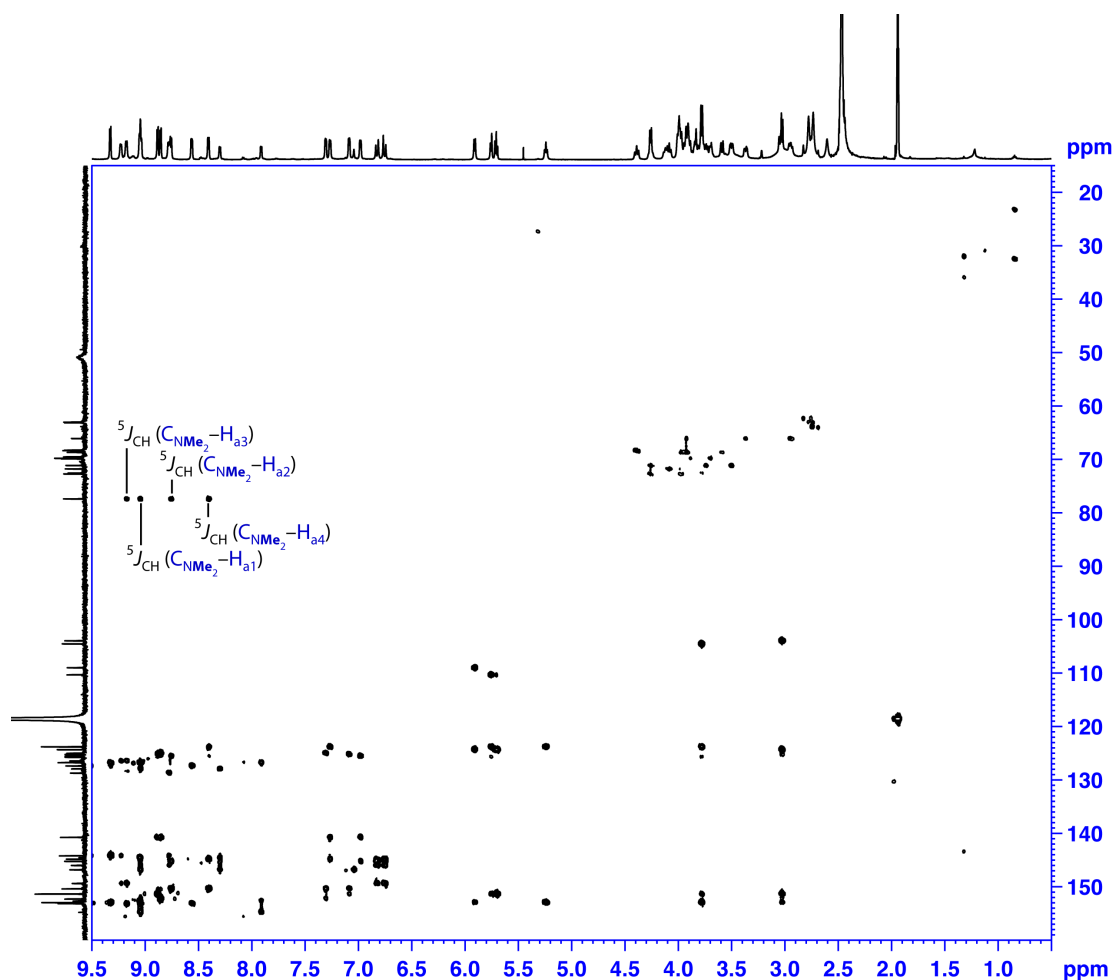


Fig S6. $^1\text{H}\text{-}^{13}\text{C}$ HMBC NMR spectrum (600 MHz, 233 K, CD_3CN) of $\text{DN50C14} \subset 2 \cdot 8\text{PF}_6$, with selected correlations shown.

Additional details as to the solution structure were provided by the ^1H - ^{13}C HMBC NMR spectrum recorded in CD_3CN at 233 K (Figure S6), which assists in the characterisation of the protons of the 1,1'-methylenebis-4,4'-bipyridinium ligand. While the NOESY spectrum (Figure S5) shows through-space correlations between the methylene group and the H_α protons, the HMBC spectrum reveals through-bond correlations between the tmeda ligand and the H_α protons, confirming their respective identities.

In combination, these comprehensive NMR spectroscopic data have allowed us to identify the ring-in-ring complex $\text{DN50C14} \subset 2 \cdot 8\text{PF}_6$ unambiguously as the dominant species present in solution and to assign the resonances in the ^1H spectrum.

S3. Variable Temperature NMR of $4 \cdot 8\text{PF}_6$

A mixture of DN50C14 and $1 \cdot 8\text{PF}_6$ in CD_3CN was analysed by ^1H NMR spectroscopy at 10 K intervals from 233 K to 293 K (Figure S7).

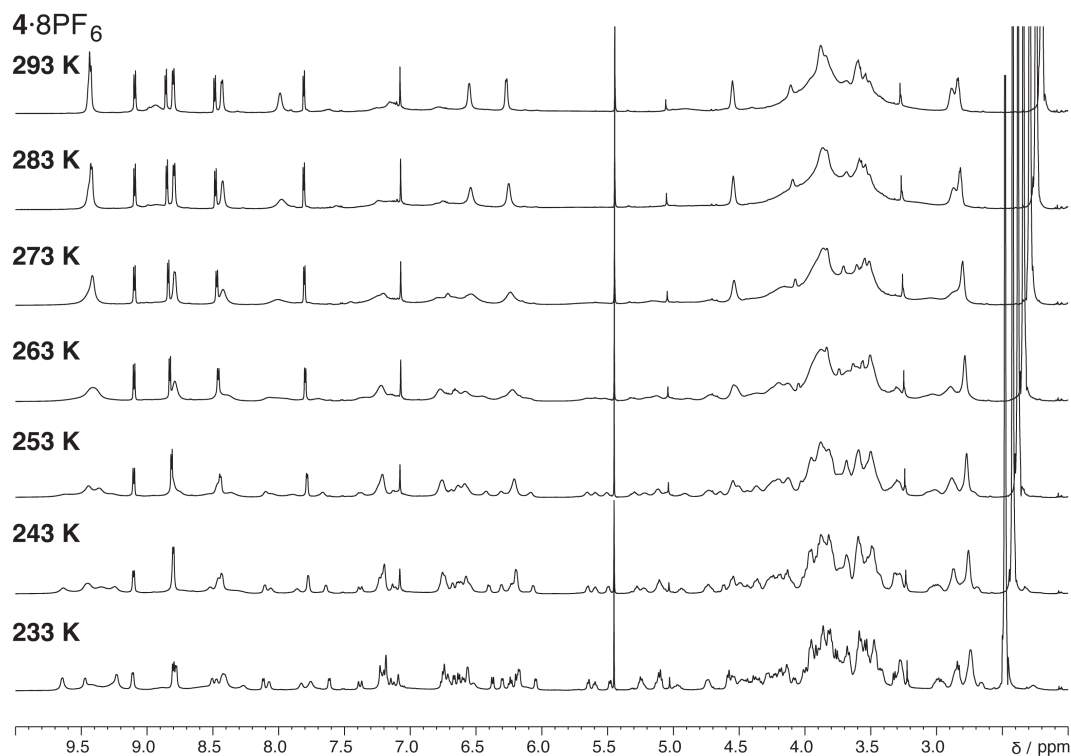


Fig S7. Stacked plot of variable temperature 600 MHz ^1H NMR spectra of a mixture of DN50C14 and $1 \cdot 8\text{PF}_6$ recorded in CD_3CN at 10 K intervals from 233 K to 293K.

It was, however, not possible to obtain a well-resolved spectrum at any of the temperatures investigated. The spectrum obtained at 233 K is reminiscent of that recorded^{S1} by Quintela *et al* for the [3]catenane **3**·4OTf·4PF₆ in CD₃CN at 233 K. This similarity, allied with the fact that a ring-in-ring complex is not formed, suggests that the [3]catenane **4**·8PF₆ is the dominant species in solution. If this is the case, the line broadening of the ¹H NMR spectrum at 233 K could be attributed to translational motion of the rings of the [3]catenane.

S4. NMR Characterisation of DN38C10 ⊂ 2·8PF₆

Attempts to isolate the ring-in-ring complex DN38C10 ⊂ 2·8PF₆ were hampered by the very poor solubility of DN38C10 in CD₃CN. It was possible to record an ¹H NMR spectrum (Figure S8) of a mixture of DN38C10 and 2·8PF₆ in CD₃CN at 233 K, however, a significant quantity of DN38C10 had precipitated from solution, affecting the stoichiometry of the mixture (see Section S1). Thus, the spectrum has notable resonances that are assigned to the free square 2·8PF₆. The remaining signals are reminiscent of those observed for the analogous ring-in-ring complex DN50C14 ⊂ 2·8PF₆, which is indicative of the assembly of DN38C10 ⊂ 2·8PF₆. The spectrum is not completely resolved, with two large broad singlets accounting for two of the protons of 2·8PF₆, an observation which suggests that formation of DN38C10 ⊂ 2·8PF₆ is not as favourable at 233 K as in the case of DN50C14 ⊂ 2·8PF₆.

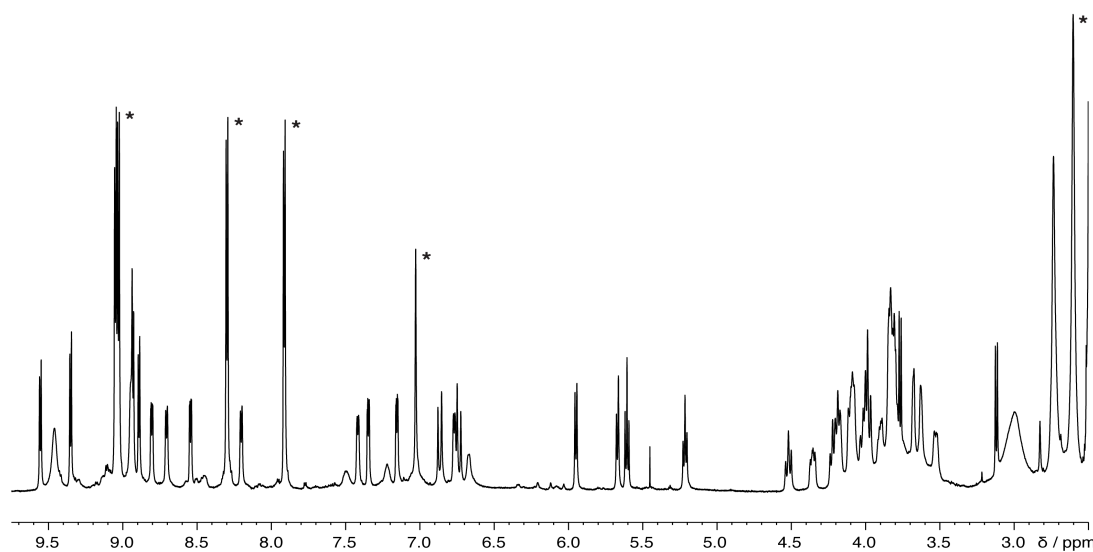


Fig S8. ¹H NMR spectrum (600 MHz, 233 K, CD₃CN) of a mixture of DN38C10 and 2·8PF₆. Peaks marked with an asterisk (*) correspond to signals for the free square 2·8PF₆.

S5. DOSY Experiments

Diffusion NMR spectroscopic experiments were performed on a Bruker Avance 800 MHz NMR spectrometer using a triple-axis gradient 5 mm TCI probe. All samples were prepared in CD₃CN solution and the temperature was regulated to 233 K. DOSY measurements were acquired using a pulsed-field gradient simulated spin echo using dipolar gradients (δ) of 3100 μ s each and a diffusion time (Δ) of 140 ms. The diffusion dimension was developed from 16 linear steps of the gradient power. Fits were obtained using Bruker Topspin v.2.1.

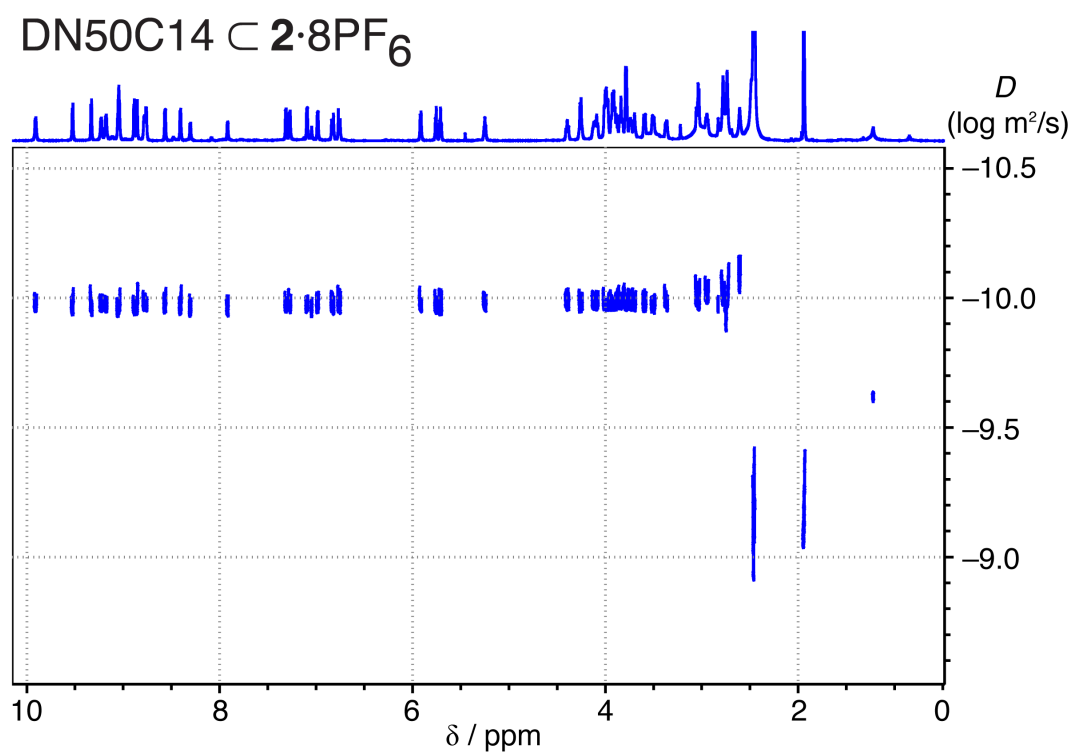


Fig S9. DOSY ¹H NMR spectrum (800 MHz, 233 K, CD₃CN) of DN50C14 C 2·8PF₆ with a diffusion coefficient of 28 nm²·s⁻¹.

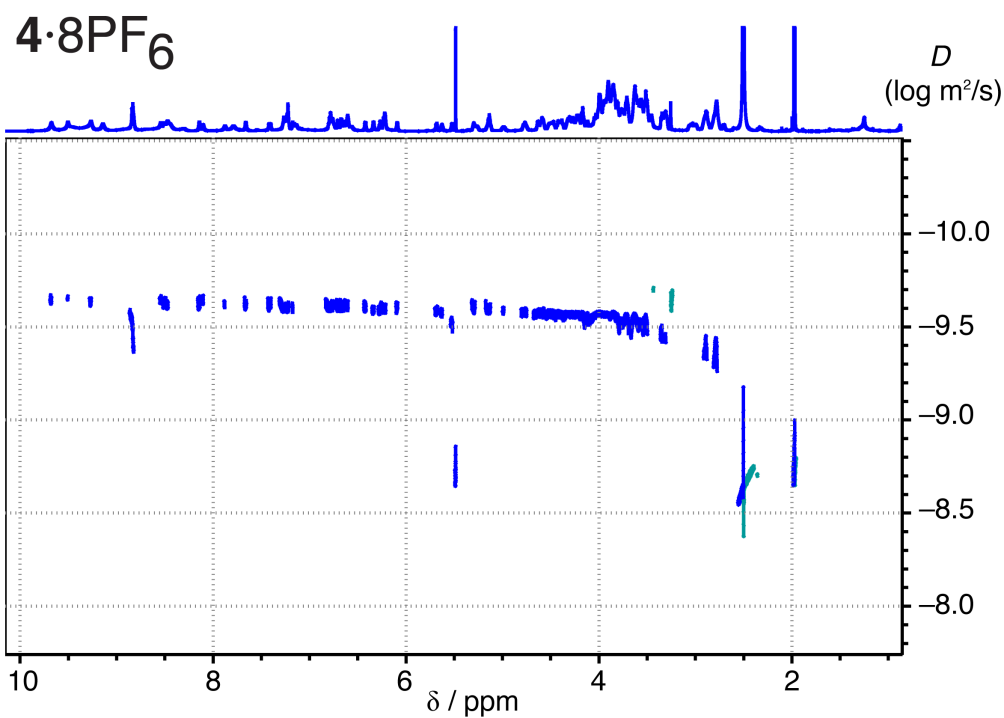


Fig S10. DOSY ¹H NMR spectrum (800 MHz, 233 K, CD₃CN) of 4·8PF₆ with a diffusion coefficient of 26 nm²·s⁻¹.

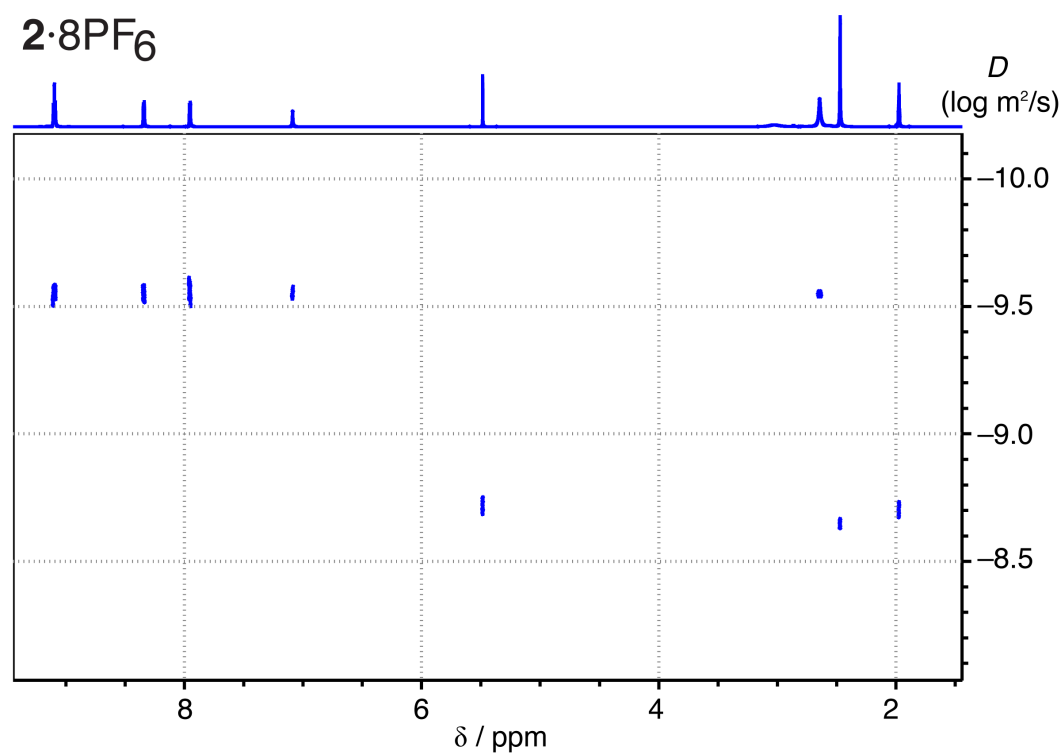


Fig S11. DOSY ¹H NMR spectrum (600 MHz, 233 K, CD₃CN) of 2·8PF₆ with a diffusion coefficient of 21.8 nm²·s⁻¹.

Diffusion constants at 233 K in CD₃CN were measured for each species. The similar values of 28 and 26 nm²s⁻¹ for DN50C14 C 2·8PF₆ and 2·8PF₆, respectively, are a result of their similar size in solution, whilst the value of 22 nm²s⁻¹ for 4·8PF₆ illustrates its larger size in solution.

S6 – UV/Vis Spectroscopy

Partial UV/Vis spectra of DN50C14 C 2·8PF₆, DN38C10 C 2·8PF₆ and 4·8PF₆ were recorded in CD₃CN and are displayed in Figure S12. The spectra all show a charge transfer band at $\lambda = 510$ nm, which is ascribed to the interaction between the bipyridinium units of the molecular squares and the dioxynaphthalene moieties of the crown ethers. Notably, the spectra of DN50C14 C 2·8PF₆ and DN38C10 C 2·8PF₆ are almost identical.

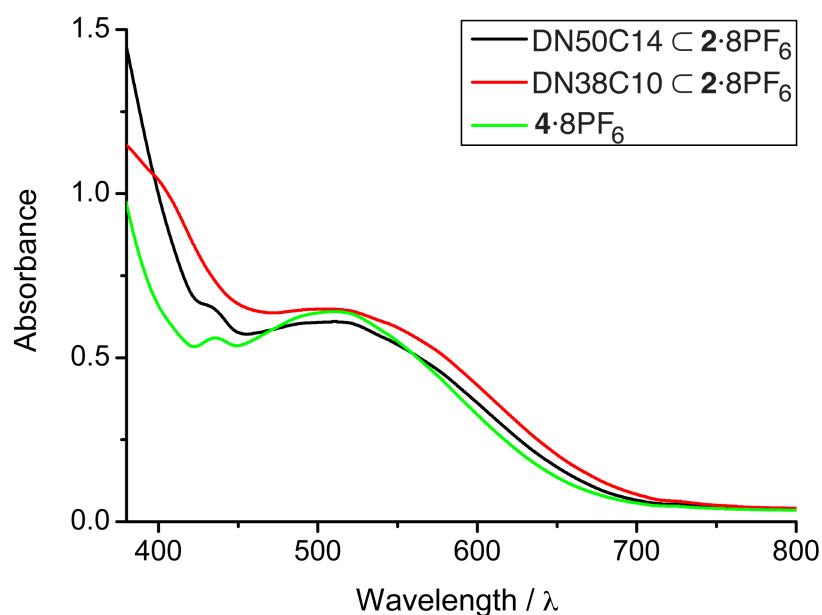


Fig S12. Partial UV/Vis spectra in CD₃CN of DN50C14 C 2·8PF₆ (12.5 mM, black line), DN38C10 C 2·8PF₆ (25 mM, red line) and 4·8PF₆ (6.25 mM, green line).

S7. Crystal Structure of 2·8PF₆

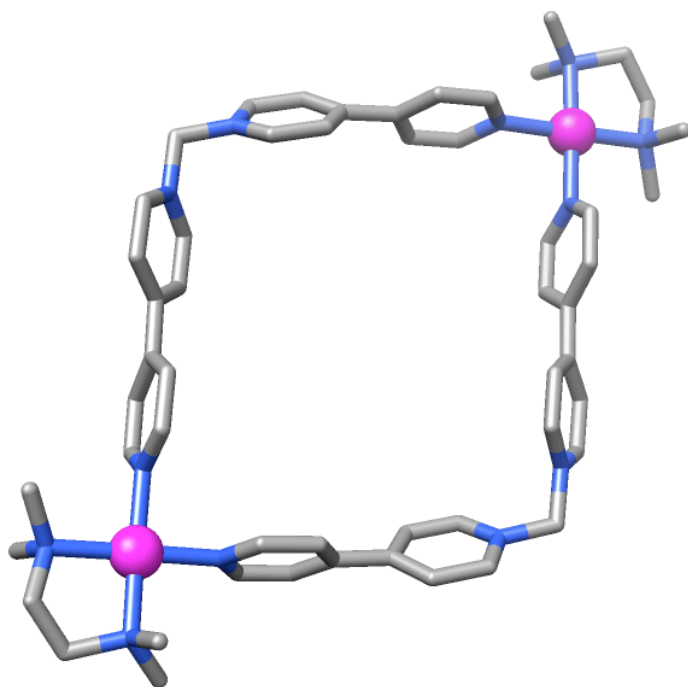


Fig S13. Tubular representation of the solid-state structure of 2·8PF₆. All counterions, solvent molecules and hydrogen atoms are removed for clarity. Carbon atoms are grey, nitrogen atoms blue and palladium cations depicted as pink spheres.

Single crystals of 2·8PF₆ were isolated during attempts to crystallise the ring-in-ring complex DN38C10 ⊂ 2·8PF₆, and subsequently could also be isolated from CD₃CN solutions of 2·8PF₆ itself, by vapour diffusion of Et₂O into the solution (Fig S13).

References

- S1. V. Blanco, M. Chas, D. Abella, C. Peinador and J. M. Quintela, *J. Am. Chem. Soc.*, 2007, **129**, 13978–13986.
- S2. R. S. Forgan, J. M. Spruell, J.-C. Olsen, C. L. Stern and J. F. Stoddart, *J. Mex. Chem. Soc.*, 2009, **53**, 134–138.
- S3. C. J. Bruns, S. Basu and J. F. Stoddart, *Tetrahedron Lett.*, 2010, **51**, 983–986.